The Impact of Synchronous Generators Excitation Supply on Protection and Relays

Gabriel Benmouyal, *Schweitzer Engineering Laboratories, Inc.*

***Abstract*—Synchronous generators have two types of operational limits: thermal and stability. These limits are commonly defined in the P-Q plane and, consequently, the point of operation of a generator should not lie beyond any of these limits. The functions that prevent the generator from infringing into the forbidden zones are known as limiters and are normally embedded in the generator Automatic Voltage Regulator (AVR). The combination of these limiters and the nature of the AVR itself will have an impact on some generator protective functions like the loss-of-field (LOF) or out-of-step protection. The purpose of this paper is not to review generators' protection principles, because this has been done extensively elsewhere, but rather to revisit the basic physical and engineering principles behind the interaction between a synchronous generator AVR and its associated limiters and some of the generator protective functions. We review the technology of the limiters embedded in a generator AVR. In LOF coordination studies, the steady-state stability limit (SSSL) used most often has been traditionally based on a generator-system with a constant-voltage excitation (or manual SSSL). In this paper, we discuss the impact of the excitation system with an AVR or a power system stabilizer (PSS) on the generator stability limits. A new numerical technique is introduced to determine the stability limits of a generator-system where the excitation supply could be regulated using either an AVR or an AVR supplemented by a PSS.**

I. Generator Thermal and Steady-State Stability Limits

There are three types of thermal limits ([1]–[4]) in a generator: the armature current limit that is directly related to the generator rated power, the field current limit, and the end core limit. The steady-state stability limit is a direct consequence of the power transfer equation between a generator and the network that it is supplying. These different limits are reviewed in the next section.

A. Generator Thermal Operational Limits

In Fig. 1, the three types of thermal limits found on a generator are represented. Assuming that the power is measured in per-unit (p. u.) values, a half-circle with unit radius represents the generator theoretical maximum capability (GTMC). This limit is caused by the armature current ohmic losses and corresponds simply to the generator MVA rating.

The end-core limit is a consequence of the end-turn leakage flux existing in the end region of a generator. The end-turn leakage flux enters and leaves in a direction perpendicular to the stator lamination. Eddy currents will then flow in the lamination and will be the cause of localized heating in the end region. In overexcited mode, the field current is high and as a consequence the retaining ring will get saturated so that the end flux leakage will be small. In the underexcited mode, the field current will be reduced and the flux caused by the armature current will add up to the flux produced by the field current. This will exacerbate the end-region heating and will severely limit the generator output. The end-core limit depends upon the turbine construction and geometry. The limitation could be particularly severe for gas turbines, yet could be nonexistent for hydro units as shown in Fig. 1; steam units would have a limiting characteristic in the middle [1].

The field and armature current limits are dependant upon the generator voltage. All three limits are dependant upon the generator cooling system. For hydrogen-cooled generators, the most tolerant limit will occur at the maximum coolant pressure (see Fig. 2).

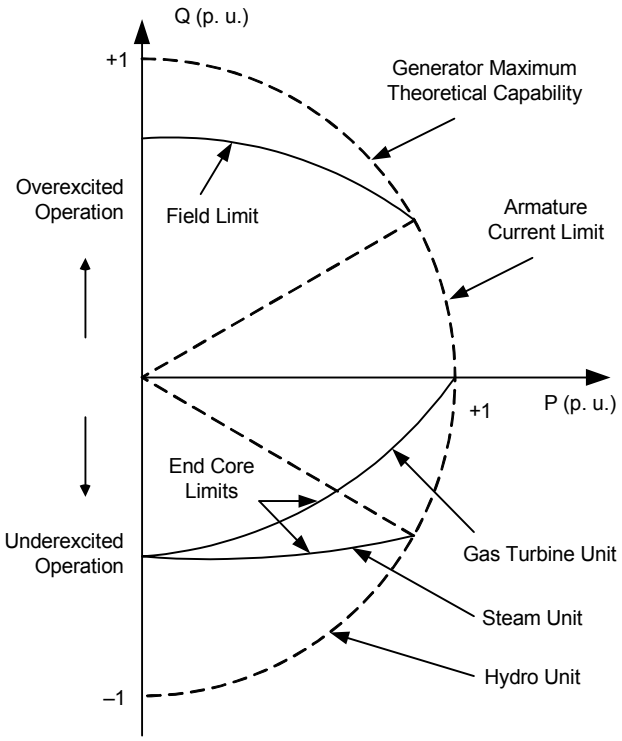

Fig. 1. Generator operation thermal limits

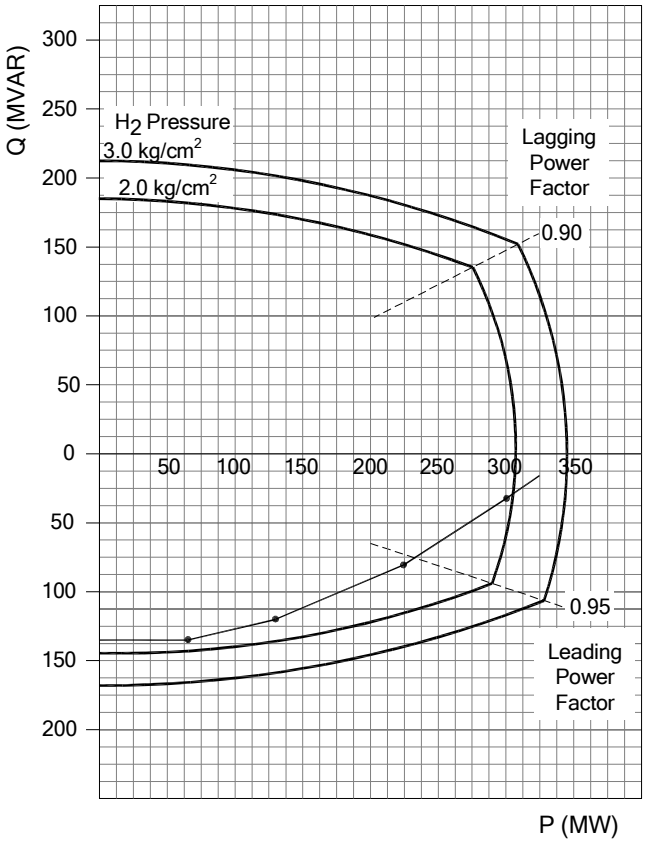

Fig. 2. Capability curve at nominal voltage of a 312 MW, 347 MVA, 20 kV, 0.9 PF, 3600 rpm, 60 Hz, hydrogen-cooled steam-turbine generator

B. Classic Steady-State Stability Limit of Round Rotor Generator

The steady-state stability limit of a generator determines the region in the P-Q plane where the generator operation will be stable in a normal mode of operation. Normal mode of operation is defined here as a mode where only small and minor disturbances are occurring on the network, as opposed to major disturbances such as faults, significant addition of load, or loss of generation. The steady-state stability limit is used by protection engineers in some coordination studies and for the adjustment of the under-excitation limiter (UEL) function in the AVR [1, 5].

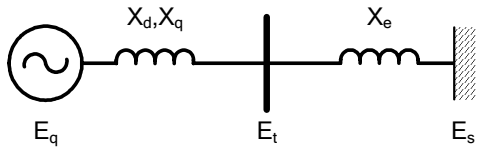

Fig. 3. Elementary generator-system

The manual SSSL is derived for a generator-system corresponding to Fig. 3, where the generator supplies its load to an infinite bus through a line with impedance X_e. The generator excitation is assumed to be supplied with a constant voltage. The power transfer equation for a salient-pole machine is provided in steady state by the conventional formula:

$$P = \frac{E_q E_s}{X_d + X_e}\sin\delta + E_s^2 \frac{X_d - X_q}{2(X_d + X_e)(X_q + X_e)}\sin 2\delta \quad (1)$$

In this last equation, the angle δ is the angle between the generator internal voltage E_q and the infinite bus voltage E_s. It is a well-established principle that the generator stability limit is reached when the derivative of the real power P with respect to the angle δ becomes equal to zero.

$$\frac{\delta P}{\delta t} = \frac{E_q E_s}{X_d + X_e}\cos\delta + E_s^2 \frac{X_d - X_q}{(X_d + X_e)(X_q + X_e)}\cos 2\delta = 0 \quad (2)$$

Trying to solve (2) will lead to non-linear equations, and there is no algebraic equation for the SSSL. The problem can be simplified, however, by considering a round-rotor machine, for which X_d equals X_q equals the synchronous reactance X_s so that the power transfer equation becomes:

$$P = \frac{E_q E_s}{X_s + X_e}\sin\delta \quad (3)$$

In this case, the stability limit is reached when the angle δ reaches the value of 90°. A circle with a center and radius, as shown in Fig. 4, provides the stability limit under manual operation in the P-Q plane [1].

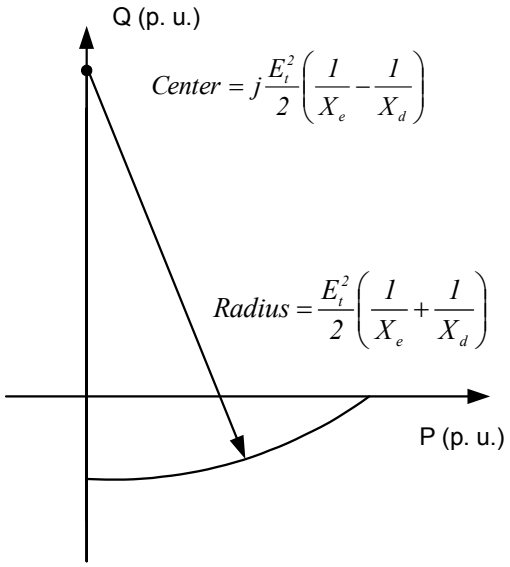

Fig. 4. Manual SSSL circle for generator system with constant excitation

Fig. 5 in the per-unit P-Q plane provides a better picture of the practical issues associated with the manual SSSL. A half-circle of radius 1 and center (0,0) has been drawn and represents the already defined GTMC limit. The generator operating point will normally be inside the GTMC circle or on its circumference in the allowed region, so that the generator operation does not exceed the generator ratings.

Assuming the generator terminal voltage E_t to be 1.0 pu, the intersection of the manual SSSL curve with the imaginary axis is equal to $-1/X_d$. This indicates that for a generator with X_d greater than one, the manual SSSL will automatically infringe into the GTMC circle and the generator will become unstable when it becomes heavily underexcited. The intersection with the real axis is at point $1/\sqrt{(X_d+X_e)}$. This indicates that as the value of the external line impedance X_e increases, the manual SSSL becomes closer to the GTMC circle. With both X_d and X_e being equal to one, the SSSL and the GTMC

circle coincide. There are high values of X_e for which the generator could not supply its rated power without becoming unstable: the manual SSSL infringes inside the GTMC limit.

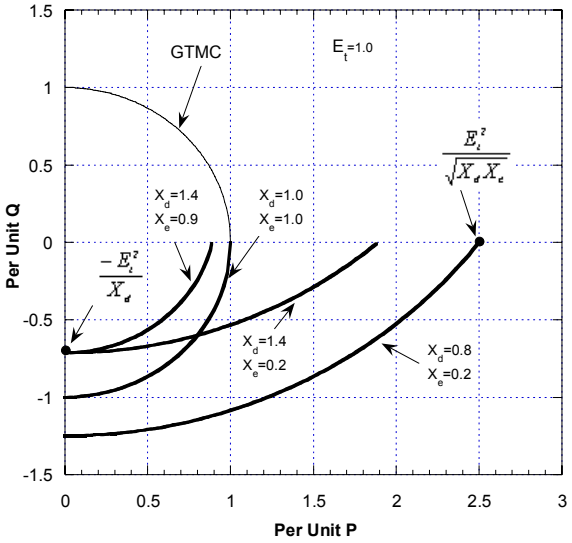

Fig. 5. Manual SSSL with respect to the GTMC circle

1) Impact of the Saliency on the Manual SSSL

As already noted, when saliency is taken into account, there is no algebraic equation available to plot the manual SSSL circle. This is probably the reason why saliency is never taken into account. However, the SSSL of a salient pole generator can be determined numerically by solving numerically (2). A program has been written to solve numerically (1) and (2). Fig. 6 shows the SSSL of both a salient pole and round-rotor generators with the indicated characteristics. One can see that the difference between the two curves lies only in the area close to the imaginary axis where the point of intersection is at point $-1/X_q$ for the salient pole generator rather than $-1/X_d$ for the round-rotor generator. Therefore the difference between the two SSSL curves should be considered as negligible for practical purposes.

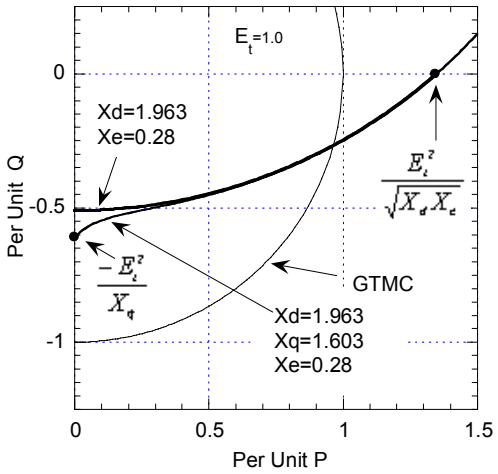

Fig. 6. Impact of the saliency on the manual SSSL

II. The Synchronous Generator Excitation System

A. The Nature of the Generator Excitation

The primary function of a synchronous generator excitation system is to regulate the voltage at the generator output. In a synchronous machine, the rotating magnetic field necessary to induce voltage in the stator windings is produced by the dc current that circulates in the rotor or field winding. A synchronous generator excitation voltage is the voltage measured at the generator terminals when the load current is equal to zero. Its rms value is proportional to the current flowing in the rotor winding:

$$E_f = \frac{\omega L_{af}\, i_f}{\sqrt{2}} \tag{4}$$

This dc current flowing in the rotor winding is produced by the excitation system. At steady state, it is equal to the dc excitation voltage supplied to the rotor winding divided by the winding resistance:

$$i_f = \frac{E_{fd}}{r_f} \tag{5}$$

The field winding has a self-inductance L_{ff}. A fundamental characteristic of a synchronous generator is the direct-axis open-circuit transient time constant T_{do}', the ratio of the field self inductance over its dc resistance:

$$T_{do}^{'} = \frac{L_{ff}}{r_f} \tag{6}$$

This time constant, which has the value of a few seconds, typically indicates that the voltage at the synchronous generator terminals cannot be changed instantaneously; in other words, the current in the field winding varies according to the field open-circuit time constant.

B. The Automatic Voltage Regulator

This paper focuses on present day excitation static systems such as shown in Fig. 7. In these systems, the input power for the static exciter is commonly derived from the machine terminals. A step-down transformer (excitation transformer PPT) feeds a three-phase controlled rectifier bridge that converts ac voltage into dc voltage. The dc output is connected to the machine field winding by brushes and collector rings.

In automatic mode, a voltage set point in introduced in the summing point of the AVR. This voltage set point is compared to the generator output voltage measurement and the comparison produces an error signal that adjusts the timing of the firing of the silicon-controlled rectifiers until the output voltage becomes equal to the voltage set point. In steady state, the generator output voltage is equal to the voltage set point. In manual mode, either the level of the generator output voltage, or the field current level (as shown Fig. 7) is under the manual control of the operator. Although still applied on some old machines, manual control of the excitation systems is not recommended by bodies like NERC in North America, given the drawbacks and shortcomings that this mode of operation will entail.

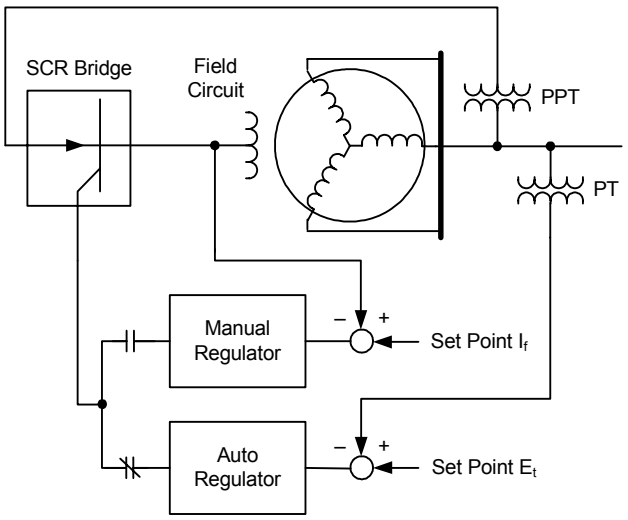

Fig. 7. AVR principle with self-exciting generator

Fig. 8 represents the generic model of a static excitation as provided among others by [11]. Such models are intended as guidelines for stability studies. V_{ref} is the voltage setting, V_c is the voltage measurement from the generator terminals. The difference between these two quantities constitutes the basic error signal. Provision is made for additional error signals at the AVR summing point. V_s is the error signal from a PSS. V_{UEL} is the error signal from an under excitation limiter to be described later. In the excitation system of Fig. 8, an auction is taking place between some signals; in other words, an HV gate will pick out the input signal that has the highest level when a LV gate picks out the signal that has the smaller one. When used, this auctioneering action allows some signals to take control of the AVR loop. As an example, following the AVR summing point, if the error signal from the UEL circuit is larger than the error signal from the summing point, priority is given to the UEL signal that takes control of the AVR loop. The output of the AVR is the voltage supplied to the field circuit. This voltage is bounded and is of primary importance. The maximum voltage supplied by the excitation system is commonly called the AVR ceiling. In small signal analysis, as described later, a static AVR can simply be represented by a gain with a time constant as shown in Fig. 9.

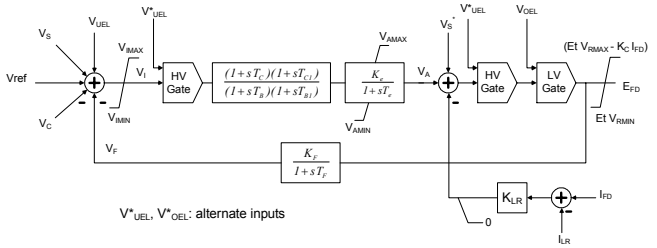

Fig. 8. IEEE type ST1A excitation system

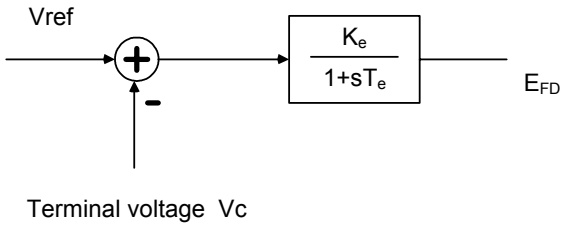

Fig. 9. Simplified representation of a static excitation system

III. Protective Limiters Embedded in the AVR

Generator thermal protective functions are embedded in the AVR by way of limiters. Using limiters means that these functions do not trip the generator, but keep it away from operating outside the boundaries indicated in Fig. 1. There are usually three limiters that can be implemented in the AVR: the underexcitation (or minimum) limiter (UEL or MEL), the overexcitation limiter (OEL), and the volt/hertz limiter (VHL). The UEL prevents the generator from operating below the end-core limits shown in Fig. 1. It could also, depending upon which is the most constraining, prevent the generator from operating below the SSSL. The OEL prevents the generator from operating above the field limit of Fig.1. The VHL prevents the generator from operating above a volt/hertz maximum threshold. The next section presents examples of means for implementing these different limiters.

A. The Underexcitation Limiter Implementation

1) The Control of the Generator Reactive Power

Consider the system in Fig. 10 representing a generator connected to an infinite bus through an impedance Z_e. Assume that the infinite bus has unity voltage, the impedance is 15 percent and the generator voltage takes the three values 0.95, 1.0, and 1.05 p. u. The circle diagram of Fig. 11 represents the relationship between the real and reactive power at the generator for all three cases. For each case, the circle has the next coordinates for the center and next radius value:

$$\text{Center} = (0, E_t^2 / Z_e)$$
$$\text{Radius} = \frac{E_t E_s}{Z_e} \tag{7}$$

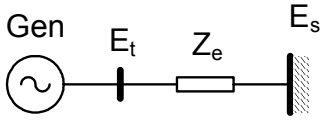

Fig. 10. Generator supplying an infinite bus

Examining Fig. 11, one can see that when the generator voltage is above the system voltage, the generator produces positive VARs. When the generator voltage is equal to the system voltage, the generator has a power factor close to one (it does not produce any VARs at all). Finally, when the generator voltage is below the system voltage, the generator will absorb VARs.

This observation indicates that when a generator goes underexcited to the point that the negative VARs might get be-

low the generator capability limit, the solution is to increase the generator output voltage until the absorbed VARs get above the limit. This is precisely what an UEL will do by producing a positive error signal that will be supplied to the AVR summing point when it requires the generator AVR to increase the output voltage.

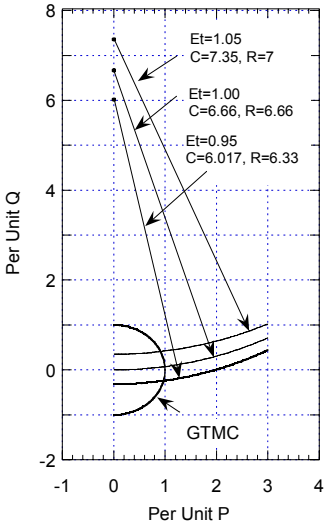

Fig. 11. Control of the generator reactive power by its output voltage

2) The Underexcitation Limiter Embedment in the AVR

Consider the UEL model (type UEL2) as shown in Fig. 12. In this model, k_1, k_2, KUP, KUV and KUQ are settings introduced by the user. T_{UV}, T_{UQ} and T_{UP} are the circuit time constants that determine its dynamics. This circuit comes from the recommended models in [8]. The UEL static or steady-state characteristic can be determined by setting the Laplacian operator "s" to zero and by looking at the condition when the error signal from the UEL circuit will be zero [1]. This condition is provided by:

$$P E_t^{-k1} KUP - E_t^{k2} KUV - Q E_t^{-k1} KUQ = 0 \tag{8}$$

Expressing Q as a function of P, we obtain:

$$Q = P \frac{KUP}{KUQ} - E_t^{(k1+k2)} \frac{KUV}{KUQ} \tag{9}$$

Equation (9) is the equation of a straight line as shown in Fig. 13 and represents the UEL characteristic in the P-Q plane. When the generator operating point gets below the line segment, the UEL will produce a positive error that will be supplied to the AVR summing point. This positive error will, in turn, have the effect of increasing the voltage setting or AVR voltage reference so that the generator terminal voltage will also increase until the generator operating point goes above the UEL limit straight-line characteristic. Later, we will show how the exponent (k_1 + k_2) allows having coordination with the LOF function in the P-Q plane that is not affected by the generator voltage.

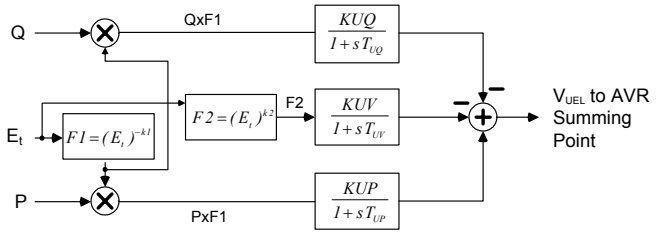

Fig. 12. Example of an UEL2 type straight-line underexcitation limiter

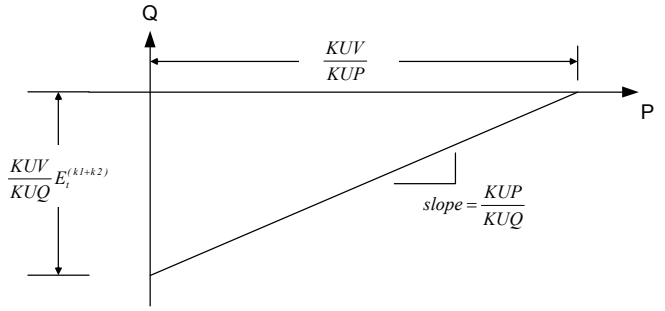

Fig. 13. UEL2 type straight-line characteristic

Reference [8] describes two additional UEL characteristics, one circular (type UEL1) and one multi-segment straight line (type UEL3), working on the same principles as type UEL2.

B. The Overexcitation Limiter Implementation

The OEL purpose is to essentially limit the field current value so that the generator operating point does not go above the field current limit of Fig. 1. Fig. 14 provides an example [18] of an OEL providing an error signal to the AVR summing point.

When the field current I_{fd} is below some pickup value, shown here to be 1.05 times the field current at full load, a negative signal through path "a" will drive the integrator (1/s) to its lowest value –A and this will provide a null error signal to the AVR summing point.

When the field current goes above the pickup value, a positive signal through path "b" will be supplied to the integrator so that a negative error will be supplied to the AVR summing point. This negative error signal will reduce the field voltage E_{fd} until the field current goes below the pickup value. For a step current increase above the pickup, [18] provides the time for the field current to start to be a limiter:

$$t = \frac{A}{G_2 G_3 (I_{fd} - 1.05 I_{fd\ rated})} \tag{10}$$

Equation (10) is the equation of an inverse curve. The parameters can be adjusted so that the inverse characteristic will coordinate with the generator field capacity that is defined as a time-inverse current curve by standards [9].

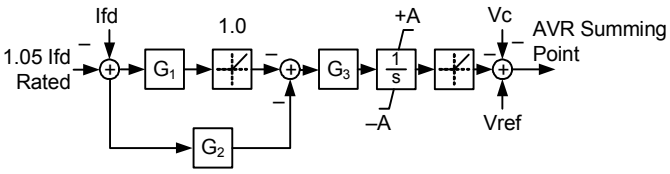

Fig. 14. Example of an OEL model

C. The Volt/Hertz Limiter Implementation

Fig. 15 represents an example of a VHL model [2] that will provide an error signal to the AVR summing point. This example assumes that a measurement of the generator terminal voltage E_t and frequency "freq" are available to the circuit. When the ratio of generator output voltage divided by the frequency goes above a maximum volt/hertz threshold shown here as 1.07 p. u., the difference is integrated and a negative signal is sent to the AVR summing point. The negative signal reduces the generator output voltage until the voltage to frequency ratio goes below the threshold. When the difference becomes negative, the integrator is reset to zero so that the error signal becomes null. Therefore, a VHL will change the generator output voltage but will have no effect on the generator frequency.

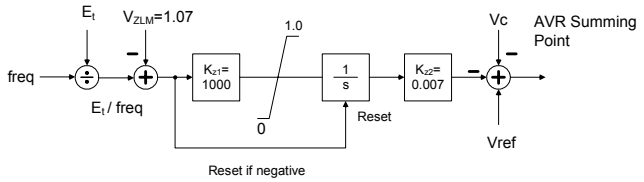

Fig. 15. Example of a volt/hertz limiter model

IV. The Impact of the AVR on the Generator-System Steady-State Stability Limit

The only simple formula hitherto available to protection engineers for plotting the SSSL of a generator-system is for the case of a generator with constant excitation. This limit type was assumed to be conservative enough that it could be applicable without any restriction to generator-systems with AVR or PSS [5]. In the next paragraphs, we will introduce a new technique to derive the small-signal stability limit of a generator-system with either an AVR or an AVR-PSS combination. Before presenting the new technique, we will introduce basic notions of small signal analysis (SSA) and stability (SSS).

A. Fundamental Notions of Generator Small Signal Stability Using the Classical Generator Model

The simplest (and approximate) representation of a generator is the so-called classical model [2], consisting of a constant voltage source behind the generator transient direct axis reactance, as shown in Fig. 16.

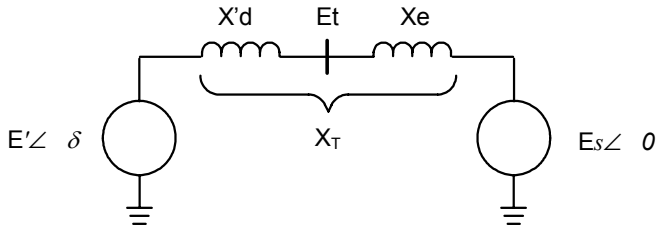

Fig. 16. Elementary power network with classical representation of generator

In the per unit system, because the rotor speed is equal to one, the power P is equivalent to the electrical torque and they are both provided by the classical power transfer equation:

$$T_e = P = \left(\frac{E' E_s}{X_T}\right)\sin\delta_0 \tag{11}$$

A small increment of the electrical torque around the quiescent point of operation can be expressed as:

$$\Delta T_e = \frac{\Delta T_e}{\partial\delta}\Delta\delta = \left(\frac{E' E_s}{X_T}\right)\cos\delta_0(\Delta\delta) \tag{12}$$

Equation (12) can be otherwise expressed as:

$$\Delta T_{sync} = K_1 \Delta\delta \tag{13}$$

with K_1 equal to:

$$K_1 = \left(\frac{E' E_s}{X_T}\right)\cos\delta_0 \tag{14}$$

Because in (13), the electrical torque variation is proportional to the variation of the generator internal angle δ, this electrical torque type is called the synchronous torque. Only the synchronous torque is apparent with the simplistic classical model of a synchronous generator. In reality, another electrical torque exists in a machine that is proportional to the speed variation of the machine. This electrical torque is called the damping torque and can be expressed as:

$$\Delta T_{damp} = K_D \Delta\omega \tag{15}$$

The total electrical torque produced by the synchronous machine is the sum of the synchronous and damping torques and is equal to:

$$\Delta T_e = \Delta T_{sync} + \Delta T_{damp} = K_1 \Delta\delta + K_D \Delta\omega \tag{16}$$

The dynamic equation of the machine rotor corresponds to the acceleration law of the rotating bodies and can be expressed as:

$$s\Delta\omega = \frac{1}{M}(\Delta T_m - \Delta T_{sync} - \Delta T_{damp}) \tag{17}$$

$$s\Delta\delta = \omega_0 \Delta\omega \tag{18}$$

In the two previous equations, we have:

ΔT_m: variation of the mechanical power input to the generator in pu

H: inertia constant, seconds

M: inertia coefficient = 2H, seconds

ω_0: base rotor electrical speed in radians per second (377 rad/s)

Given equations (13), (15), (17), and (18), the next block-diagram shown in Fig. 18, represents the dynamics of the elementary power system of Fig. 16.

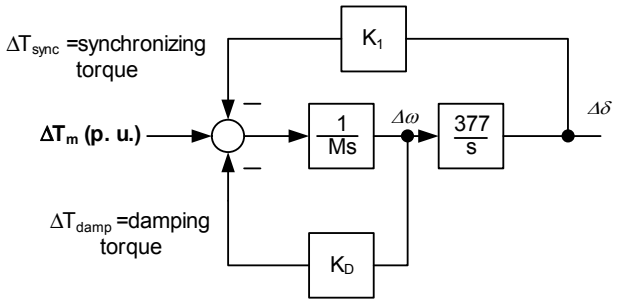

Fig. 17. Simplest possible representation of an elemental power system

Using Δω and Δδ as the state variables, we can model the elementary power system dynamics using state-space representation by the next matrix equation, as taught by modern control theory [2]:

$$\frac{d}{dt}\begin{bmatrix}\Delta\delta\\ \Delta\omega\end{bmatrix}=\begin{bmatrix}0 & \omega_0\\ -\frac{K_1}{M} & -\frac{K_D}{M}\end{bmatrix}\begin{bmatrix}\Delta\delta\\ \Delta\omega\end{bmatrix}+\begin{bmatrix}0\\ \frac{1}{M}\end{bmatrix}\Delta T_m \qquad (19)$$

This system matrix equation in the state-space corresponds to the general form:

$$\overset{o}{x} = A\,x + B\,u \qquad (20)$$

where x is the state vector, A is the state matrix, B is the control or input matrix, and u is the input or control vector. For the purpose of establishing the system output vector y, two additional matrices, C and D, are commonly defined. They are:

$$y = C\,x + D\,u \qquad (21)$$

In (21), C is defined as the output matrix and D is defined as a coefficient matrix. For the purpose of assessing the small signal stability of the system, we will discuss only the state matrix A.

The characteristic equation of the state matrix A is expressed by:

$$s^2 + \frac{K_D}{M}s + \frac{K_1\omega_0}{M} = 0 \qquad (22)$$

By identification with the classical parameters of a second order system given as:

$$s^2 + 2\zeta\omega_n s + \omega_n^2 = 0 \qquad (23)$$

The undamped natural frequency ω_n and the damping ratio ζ are found to be:

$$\omega_n = \sqrt{\frac{K_1\omega_0}{M}}\ \text{rad/s} \qquad (24)$$

$$\zeta = \frac{1}{2}\frac{K_D}{\sqrt{K_1 M\omega_0}} \qquad (25)$$

The two characteristic equation roots or system are plotted in Fig. 18.

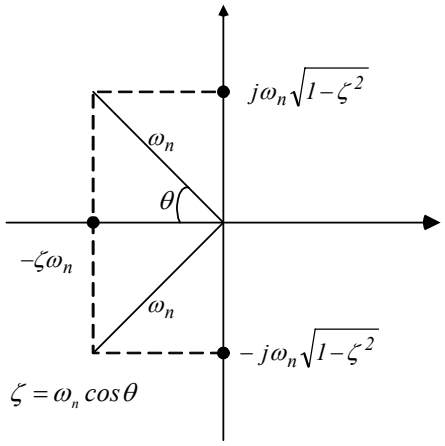

Fig. 18. Location of characteristic equation roots

The roots of the characteristic equation are identical to the state matrix A eigenvalues. For the system to be stable, both roots of the characteristic equation have to lie in the left-hand side of the complex plane as shown in Fig. 18. This implies that the undamped natural frequency ω_n and the damping factor ζ have to be positive. This, in turn, implies that the synchronizing and damping torque values have to be positive. If one of the two electrical torques becomes negative, the system will be unstable. The situation is illustrated in Table I, which displays the variation of the internal angle δ depending upon the sign of K_1 and K_D and following an impulse change of 5 percent of the mechanical torque ΔT_m.

TABLE I
INTERNAL ANGLE RESPONSE TO A 5% IMPULSE OF MECHANICAL POWER ΔT_M

	$K_D > 0$	$K_D < 0$
$K_1 > 0$	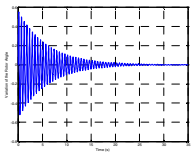	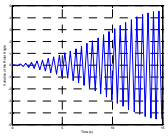
$K_1 < 0$	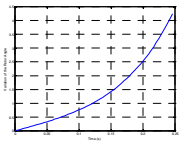	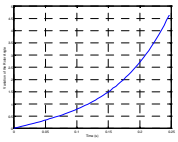

B. Small Signal Stability of a Generator With Constant Excitation Voltage

1) Advanced Generator Model

The classical model of generators has obvious limitations because it assumes that the flux linkage inside the generator is constant. We will use the more advanced model defined by Demello and Concordia in [13] to study the impact of a solid-state modern excitation system on the stability of a synchronous salient-pole generator connected to an infinite bus through a reactance X_e. The model is based on the two-axis representation of a generator, and is represented in Fig. 19.

The K parameters are identical to the ones used in [13] and are defined in Appendix A. The obvious change with respect to the classical model is that the damping torque is now produced by the generator physics.

The additional variables with respect to the classical model are:

- Δe_t: variation of the generator terminal voltage in pu
- ΔE_{fd}: variation of the field excitation voltage in pu
- $\Delta E'_q$: flux variation in the direct axis
- T_{do}': generator field open circuit time constant

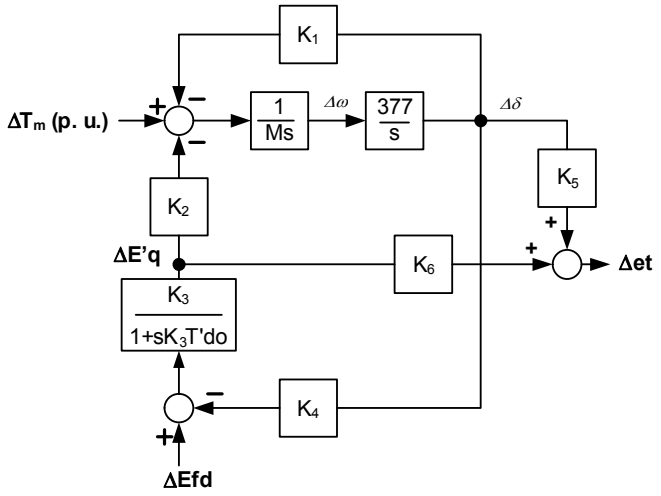

Fig. 19. Linearized model of a generator with constant excitation supply

The generator block-diagram model of Fig. 19 can be represented in the state-space using three state variables $\Delta\delta$, $\Delta\omega$, and $\Delta E'_q$ as expressed in the next matrix equation:

$$\frac{d}{dt}\begin{bmatrix}\Delta\delta\\ \Delta\omega\\ \Delta E'_q\end{bmatrix}=\begin{bmatrix}0 & 377 & 0\\ -K_1/M & 0 & -K_2/M\\ -K_3K_4/K_3T'_{d0} & 0 & -1/K_3T'_{d0}\end{bmatrix}\begin{bmatrix}\Delta\delta\\ \Delta\omega\\ \Delta E'_q\end{bmatrix}+\begin{bmatrix}0\\ 1/M\\ 0\end{bmatrix}\Delta T_m \quad (26)$$

C. Small Signal Stability Limit Using the Damping and Synchronizing Torque Limits

In the model of Fig. 19, the sum of the torques is defined as the electrical torque opposing the mechanical torque. It can be expressed, based upon Fig. 19, as:

$$\Delta T_e = (K_1 - \frac{K_2 K_3 K_4}{1 + s K_3 T'_{d0}})\Delta\delta(s) \quad (27)$$

After a few manipulations, (27) can be expressed as:

$$\Delta T_e = (K_1 - \frac{K_2 K_3 K_4}{1 - s^2 K_3^2 T'^2_{d0}})\Delta\delta(s) + (\frac{K_2 K_3^2 K_4 T'_{d0}}{1 - s^2 K_3^2 T'^2_{d0}})s\Delta\delta(s) \quad (28)$$

Obviously, the electrical torque contains a synchronizing component proportional to the angular deviation and a damping component proportional to the derivative of the angular deviation or speed. After s is given the value $j\omega$, the two component can be expressed as:

$$\Delta T_{e\_sync} = K_1 - \frac{K_2 K_3 K_4}{1 + \omega^2 K_3^2 T'^2_{d0}} \quad (29)$$

$$\Delta T_{e\_damp} = j\omega\frac{K_2 K_3^2 K_4 T'_{d0}}{1 + \omega^2 K_3^2 T'^2_{d0}} \quad (30)$$

In [1], the small signal stability limit of the system in Fig. 19 is determined by the condition when both the synchronizing and damping torques become zero. The small signal stability limit is therefore determined in the P-Q plane by plotting the two curves when the two synchronizing and damping torques equal zero and then by determining the area where both torques are positive. In the same reference, the synchronizing torque limit is determined by solving the next equation when $\omega = 0$:

$$\Delta T_{e\_sync}\Big|_{\omega=0} = K_1 - K_2 K_3 K_4 = 0 \quad (31)$$

The damping torque limit is determined by solving the next equation when ω is equal to the undamped frequency corresponding to (24):

$$\Delta T_{e\_damp}\Big|_{\omega=\sqrt{\frac{377K_1}{M}}} = j\omega\frac{K_2 K_3^2 K_4 T'_{d0}}{1 + \omega^2 K_3^2 T'^2_{d0}}\Bigg|_{\omega=\sqrt{\frac{377K_1}{M}}} = 0 \quad (32)$$

The damping torque equation corresponding to (32) does not have a solution because the damping torque is always positive. Therefore, the stability of the system is determined by the synchronizing torque limit only corresponding to the solution of (31).

1) New Method for Determining the Small-Signal Stability Limits Using the Eigenvalues Real Part Sign

For a simpler approach to the stability limit of Fig. 19 model than the two electrical torques limits, consider that the generator-system is stable if the eigenvalues of the A matrix have all their real part as negative. The new method dubbed "eigenvalues-based limit" consists then in determining for each value of the real power Pi in the complex plane, the corresponding value of imaginary power Qi for which all the real parts of the A matrix eigenvalues switch to negative (Fig. 20). Remember that for each pair of point (P,Q), there are different values for the K's parameters and therefore different eigenvalues for matrix A. After we scan a set of P values inside a chosen interval, the corresponding set of Q values as defined previously constitutes the small signal stability limit.

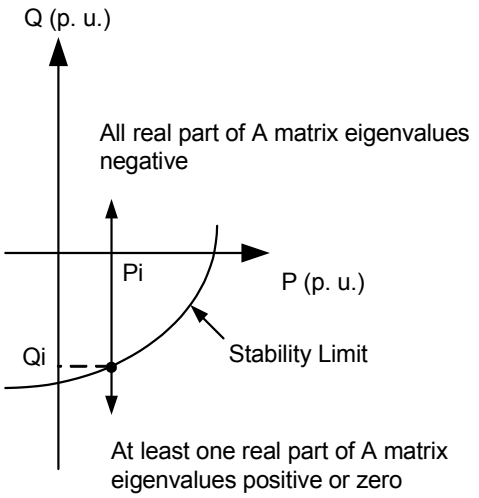

Fig. 20. Principles for determining eigenvalues-based limit

2) Equivalence Between the Manual SSSL and the Eigenvalues-Based Small-Signal Stability Limit

At this stage, we have described three methods to determine the stability limit of the generator-system of Fig. 19 with constant excitation:

1. The manual SSSL corresponding to a circle with characteristics given in Fig. 4.
2. The synchronizing torque limit only (given that the damping torque is always positive) the equation of which is provided by (31).
3. The newly defined eigenvalues-based limit.

In Fig. 21, the three stability limits obtained with the three methods are plotted for the system with constant excitation with the parameters shown. All three limits are practically identical. This demonstrates that the SSA approach together with the eigenvalues-based limit are viable for determining a generator-system stability limit.

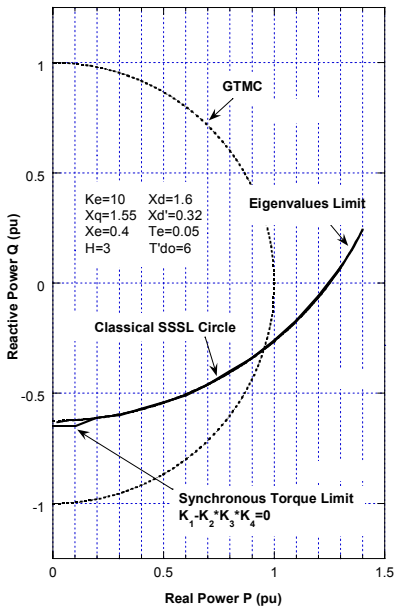

Fig. 21. Trio of stability limits for constant excitation generator system

D. Small-Signal Stability Limit of a Generator With Automatic Voltage Regulator

1) Generator Model with Automatic Voltage Regulator

All the preceding analysis has been for a generator operated under constant field voltage. When an AVR is added to the system, an additional transfer function has to be added to the system, as shown in Fig. 22. It is assumed here that a self-excited generator with a simple static excitation system is being used with transfer function:

$$\frac{\Delta E_{fd}}{\Delta e_t} = \frac{K_e}{1+sT_e} \tag{33}$$

In this last equation, K_e is the exciter gain and T_e is the exciter time constant.

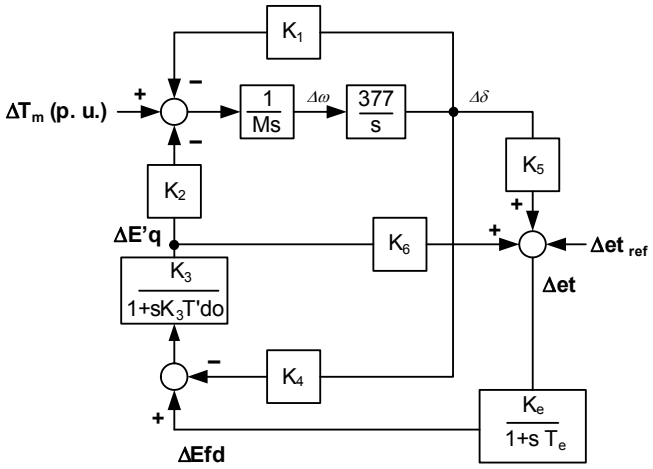

Fig. 22. Elementary power system block diagram with regulated solid-state excitation supply

The next matrix equation provides the representation of the generator system of Fig. 22 in the state-space domain:

$$\frac{d}{dt}\begin{bmatrix}\Delta\delta\\ \Delta\omega\\ \Delta E'_q\\ \Delta E_{fd}\end{bmatrix} = \begin{bmatrix}0 & 377 & 0 & 0\\ -K_1/M & 0 & -K_2/M & 0\\ -K_4/T'_{do} & 0 & -1/(K_3T'_{do}) & 1/T'_{do}\\ -(K_eK_5)/T_e & 0 & -(K_eK_6)/T_e & -1/T_e\end{bmatrix}\begin{bmatrix}\Delta\delta\\ \Delta\omega\\ \Delta E'_q\\ \Delta E_{fd}\end{bmatrix} + \begin{bmatrix}0\\ 1/M\\ 0\\ 0\end{bmatrix}\Delta T_m \tag{34}$$

2) Stability Limits Using the Eigenvalues Method

Using the eigenvalues limit method, Fig. 23 shows the stability limits of the elementary power system when the generator has an AVR and when the AVR gain is varied from zero to higher values. It is not a surprise that for an AVR gain of zero, the stability limit corresponds to the manual SSSL. As the gain increases, one can see that there is a limit to be given to the gain before the stability starts infringing inside the GTMC circle. It is a well-established principle that the AVR gain has to be limited to prevent the generator from falling into instability due to the lack of damping torque [2, 13]. Based on Fig.23, the AVR gain would have to be less than 25. Note here that the manual SSSL does not turn out to be the limit case as the gain increases. For high values of the AVR gain, the small-signal stability limit will go above the manual SSSL and will start infringing inside the GTMC limit circle.

Appendix B lists the numerical program in the MATLAB® language [19] used for plotting the small-signal stability limits in Fig. 23 and that can be used to plot further applications.

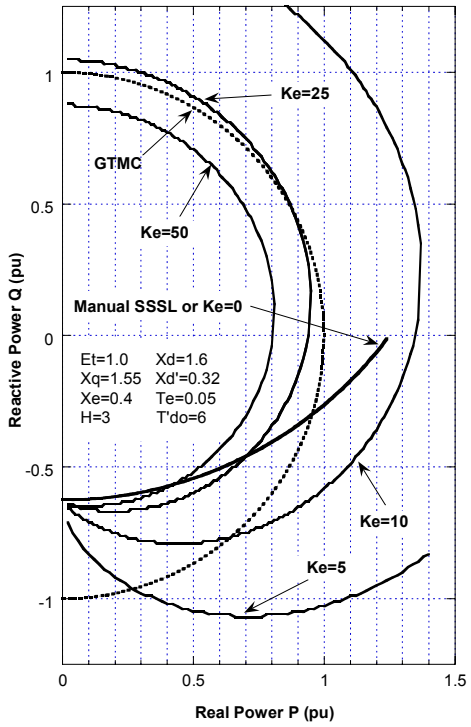

Fig. 23. Impact of the AVR gain on generator stability limit

E. Small Signal Stability Limit of a Generator System With AVR and PSS

1) Generator Model With PSS

As shown in the previous paragraph, the AVR gain has to be limited to keep the damping torque to an acceptable value. Increasing the generator transient stability requires the highest possible AVR gain to produce the highest possible excitation voltage following a major disturbance. Transient stability is defined here as the ability of the generator to maintain synchronism when subjected to a severe transient disturbance such as a fault on an adjacent transmission line. To fulfill this requirement, power engineers have developed high-speed exciters equipped with power system stabilizers (PSS). Basically, a PSS derives an error signal based on the speed of the machine and injects this error signal into the summing point of the AVR. The net effect of the PSS is to substantially increase the generator damping torque and this in turn, enables an increase in the gain.

The generator-system block diagram with the PSS added is shown in Fig. 24. The PSS transfer function consists of a gain, a high-pass filter and a phase compensation filter. In reality, a PSS could entail more complex circuitry and does not necessarily measures the speed directly [2].

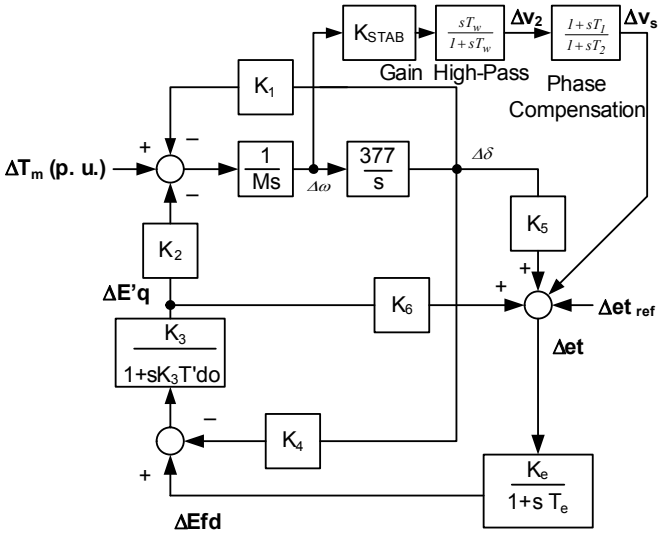

Fig. 24. Linearized elementary power system with AVR and PSS

The representation of the PSS in the state-space domain imposes the addition of two state variables as shown ΔV_s and ΔV_2 in (35).

2) Stability Limit of a Generator With a PSS Using the Eigenvalues-Based Method

The small-signal stability limit correction caused by the addition of a PSS has been studied using the eigenvalues limit method. Fig. 25 demonstrates the dramatic improvement of the system small-signal stability limit because of the PSS. Without the PSS and with an AVR gain of 50, the stability limit is infringing into the GTMC circle, as shown in Fig. 25. With a gain (K_e) of 50 and the addition of the PSS, the stability limit has moved deeply to the left of the GTMC circle and well below the manual SSSL. For the case considered, the AVR gain could be set to 200 and even higher without compromising the normal operation of the generator. As for the previous analysis with an AVR only, with the addition of a PSS, the manual SSSL does not seem to constitute a "limit-case": as the gain (K_e) increases, the small-signal stability limit will begin infringing on the GTMC circle more and more deeply.

$$\frac{d}{dt}\begin{bmatrix}\Delta\delta\\ \Delta\omega\\ \Delta E'_q\\ \Delta E_{fd}\\ \Delta V_s\\ \Delta V_2\end{bmatrix}=\begin{bmatrix}0 & 377 & 0 & 0 & 0 & 0\\ -K_1/M & 0 & -K_2/M & 0 & 0 & 0\\ -K_4/T'_{do} & 0 & -1/(K_3T'_{do}) & 1/T'_{do} & 0 & 0\\ -(K_eK_5)/T_e & 0 & -(K_eK_6)/T_e & -1/T_e & K_e/T_e & 0\\ -T_1K_{stab}K_1/(MT_2) & 0 & -T_1K_{stab}K_2/(MT_2) & 0 & -1/T_2 & 1/T_2-T_1/(T_2T_w)\\ -K_1K_{stab}/M & 0 & -K_2K_{stab}/M & 0 & 0 & -1/T_w\end{bmatrix}\begin{bmatrix}\Delta\delta\\ \Delta\omega\\ \Delta E'_q\\ \Delta E_{fd}\\ \Delta V_s\\ \Delta V_2\end{bmatrix}+\begin{bmatrix}0\\ 1/M\\ 0\\ 0\\ -1/T_w\\ TK_{stab}/T_2M\end{bmatrix}\Delta T_m \quad (35)$$

Fig. 26 shows the impact of the external impedance X_e increase of the small-signal stability. With a gain (K_e) of 150, as X_e increases from 0.4 to 0.8 p. u., one can see that the small-signal stability limit shrinks toward the left and eventually will infringe inside the GTMC limit circle for higher values of X_e. The same phenomenon has been observed with the manual SSSL of Fig. 5. Increases of the following factors contribute to the shrinking of the small-signal stability limit: the AVR gain K_e, the external impedance X_e or the AVR time-constant T_e. Reducing the following factors will lead to the same result: the generator voltage E_t, the field open-circuit time constant T'_{d0}, or the machine inertia M. As already observed, a combination of factors could exist where the small-signal stability limit could infringe deeply into the GTMC circle. The only common point between all the two types of stability limits (manual SSSL and small-signal stability limit) is that they both seem to be starting on the vertical axis on the point (0, $-1/X_d$).

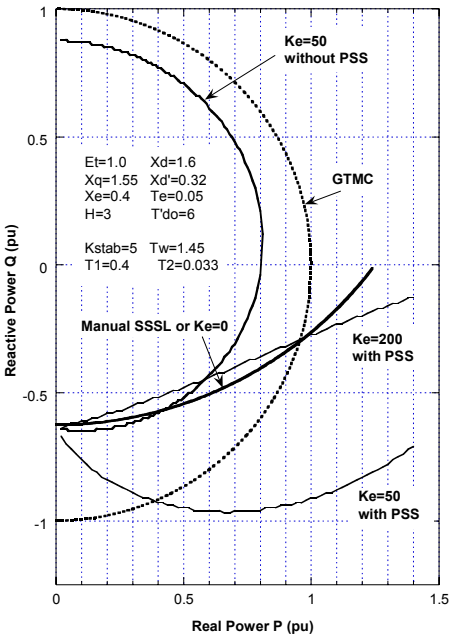

Fig. 25. Impact of PSS on Generator Stability Limit

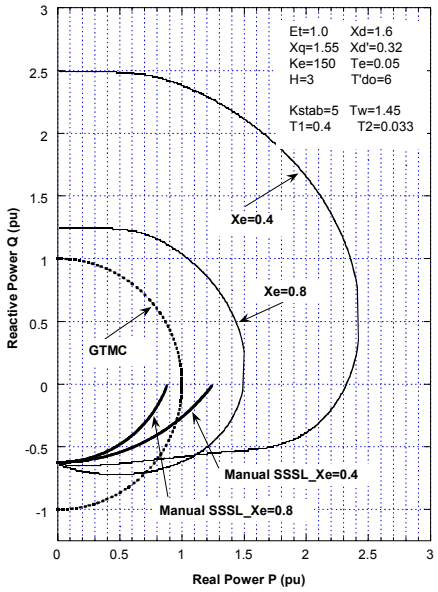

Fig. 26. Impact of Xe on generator stability limit with a PSS

V. The Excitation System Impact on Protection

A. Stability Limits Issues

Protection engineers have traditionally used the manual SSSL in their generator coordination studies because it was considered conservative enough even when an AVR or an AVR-PSS combination was added to the system. Manual operation has been and still is considered as the backup to an AVR failure. Furthermore, it has been the only simple (in the mathematical sense) limit available to protection engineers. In some instances, the manual SSSL has been presented as too conservative and counterproductive for a sound protection [3]. In some modern designs, the backup for an AVR failure could be another AVR and not manual operation. In this situation, manual operation could never occur and the traditional SSSL use loses its justification. In the preceding sections, a new technique has been tested to determine the small-signal stability limit of a generator-system without or with an AVR or with an AVR-PSS combination. From the simulation presented, one could infer that the manual SSSL, derived for a generator with constant voltage excitation, does not constitute automatically the "limit-case" to be referred to when an AVR or a PSS are considered. For reasonable values of the AVR gain and strong systems (small external impedance X_e), the manual SSSL is probably a conservative design. However, this assumption is no longer true when some factors combine together to restrain the small-signal stability limit (high AVR gain, weak system with a high external impedance X_e, etc.). Based on these considerations, there is certainly an actual requirement for simple techniques to establish a generator-system stability limit irrespective of the excitation system operation mode.

B. Volt/Hertz Issues

As described previously, a VHL is normally implemented in the excitation system. When a volt/hertz maximum thresh-

old is exceeded, this volt/hertz limiter will send a negative error signal to the AVR summation point until the generator voltage at the terminals goes back to an acceptable voltage level. The VHL does not preclude the implementation of volt/hertz protection on the generator and the step-up transformer. On the contrary, this back-up protection is desirable and recommended [5]. Bear in mind that the error signal originating from the VHL can come into conflict with the error signal from the UEL in some particular situations. As an example, in an islanding situation or during light load with a high level of charging current, the generator could be driven into an underexcited state so that the UEL will send a positive error signal to the AVR summing point. This signal will increase the generator output voltage until the generator moves out of the forbidden underexcited zone. In doing so, the voltage could go to a level high enough that the volt/hertz threshold will be exceeded and the VHL will start sending a negative error signal to lower the voltage. The outcome of this conflicting situation could be an unstable oscillation in the generator output voltage.

C. Overvoltage Issues

The primary contribution of an AVR is to keep constant the generator output voltage under a normal mode of operation. Overvoltage could occur on a transient basis during network disturbances, however. At rated frequency, the volt-hertz protection constitutes a de-facto overvoltage protection; this is probably the reason why generator overvoltage protection is not widely used in North America. A classical situation exists where overvoltage could develop without being accompanied by overfluxing: the islanding of a hydro unit or its load rejection is normally followed by a voltage build up together with an acceleration of the machine. The only protection then against machine dielectric stress is a conventional definite-time delay or inverse-time overvoltage protection.

D. Loss-of-Field Protection Issues

The main issue with the loss-of-field (LOF) protection is to ensure that when the generator goes into the underexcited region, an infringement into the LOF characteristics will not occur, with the possible consequence of the generator tripping. Two types of coordination should be considered here: static (or steady state) and dynamic coordination. Steady-state coordination corresponds to the situation where there are no disturbances on the network. Dynamic coordination corresponds to the situation where there is a disturbance and when the UEL circuit might allow the generator operating point to infringe into the forbidden underexcited region on a transient or temporary basis.

1) Steady-state Coordination

This is accomplished by coordinating the LOF characteristics with the UEL. We will assume in the next example that the manual SSSL is more constraining that the end-core limit as would happen with a hydro unit. This constitutes the worst-case scenario for the LOF protection. We limit the analysis to the conventional two-zone offset mho relay represented in Fig. 27. The coordination will be set in the P-Q plane. In the example $X_d = 1.6$, $X'_d = 0.32$ and $X_e = 0.18$.

In the R-X plane, the most important point with respect to the coordination is point "a" in Fig. 27 because it will map to the upper most position in the P-Q plane. Recall that a point in the R-X plane will map into a point into the P-Q plane following the next transformation:

$$RX(r,x) \Rightarrow PQ\left(\frac{E_t^2 r}{r^2 + x^2}, \frac{E_t^2 x}{r^2 + x^2}\right) \tag{36}$$

Assume first that the generator voltage is $E_t = 1.0$. Point "a" with coordinates $(0, -X_d\text{-}X'_d/2)$ in the R-X plane, corresponds to the following point "A" in the P-Q plane:

$$RX\left(0, -\frac{X'_d}{2} - X_d\right) \Rightarrow PQ\left(0, \frac{-E_t^2}{\frac{X'_d}{2} + X_d}\right) = PQ(0, -0.568) \tag{37}$$

The intersection of the manual SSSL with the vertical axis is:

$$PQ\left(0, \frac{-E_t^2}{X_d}\right) = PQ(0, -0.625) \tag{38}$$

As shown in Fig. 28, the intersection of the SSSL curve with the vertical axis will automatically be lower than point "A". Assume that the UEL is implemented using a straight line, the equation of which is provided by (9) with the settings shown below and assuming that k_1 and k_2 have been set each to 1:

$$Q = P\frac{KUP}{KUQ} - E_t^2\frac{KUV}{KUQ} = 0.2195\,P - 0.483\,E_t^2 \tag{39}$$

The intersection of the UEL segment with the vertical axis is chosen to be 15 percent higher than point "A". The intersection of the UEL segment with the horizontal axis is arbitrarily set to 2.2. Fig. 28 shows the overall coordination. Figs. 29 and 30 show how the coordination is maintained when the generator terminal voltage undergoes a maximum variation of 5 percent with respect to its nominal value. The moving UEL characteristic with the generator voltage Et allows keeping coordination with the mapped LOF characteristic in P-Q plane that moves also in the same fashion with the voltage variation.

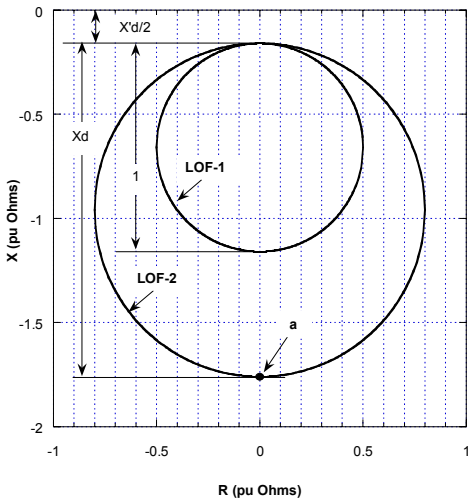

Fig. 27. Conventional offset-mho two-zone LOF characteristics

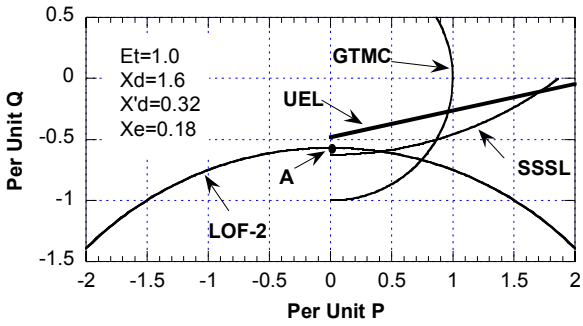

Fig. 28. Coordination of LOF and UEL for Et = 1.0

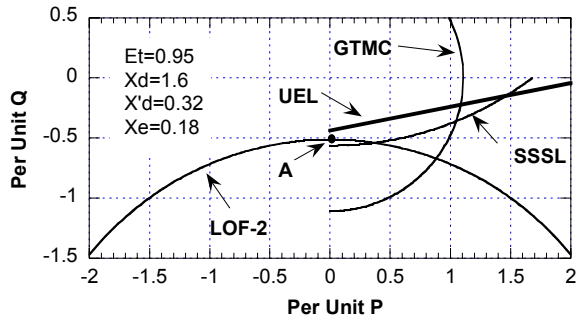

Fig. 29. Coordination of LOF and UEL for Et = 0.95

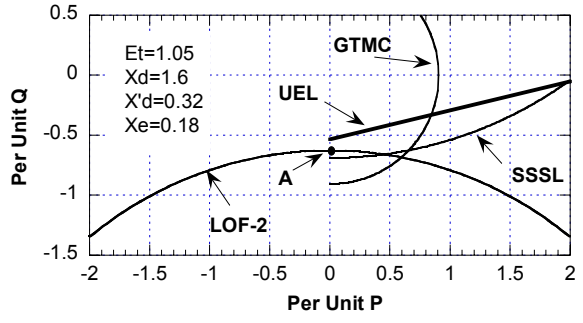

Fig. 30. Coordination of LOF and UEL for Et = 1.05

2) Dynamic Coordination

Static coordination as described in the preceding paragraph does not guarantee that the UEL will prevent the operating point from temporarily infringing into the LOF characteristics during a network disturbance. Such infringement could lead to the unit tripping. This could happen with a slow-acting UEL, the time constants of which would be too long. The only way to verify the proper dynamic coordination is by simulations [3], [17].

E. Out-of-Step Protection Issues

Generator out-of-step protection responds to the disturbances resulting from a major event like a line fault or a loss of generation. This type of protection should recognize whether the subsequent power swing is stable. Normally, the unit will trip after detecting an unstable swing. High-speed static excitation systems substantially improve the transient stability of a power network and, in many cases, contribute to the stability of the power system, as compared to less advanced or constant voltage excitation. Therefore, the main impact of the generator excitation system is on the dynamic response of the generator during a network disturbance and consequently the trajectories of the power swings. These trajectories could, in turn, affect the out-of-step relay's settings. In view of these considerations, we can infer that modeling of the excitation system should be complete and accurate before performing out-of-step simulations using programs like EMTP or Transient Stability Programs.

VI. Conclusions

1. Limiters embedded in generators AVR do not trip the unit but prevent the generator from operating in operation zones that are thermally dangerous to the machine.
2. An underexcitation limiter is normally embedded in the generator AVR and prevents the generator from operating on the forbidden underexcited region by sending an error signal to the AVR. This error signal in turn increases the AVR voltage reference so that ultimately the generator output voltage will be increased. The consequence of an UEL taking action is therefore to increase the generator output voltage.
3. A volt/hertz limiter could be embedded in the generator AVR. When called upon, it normally sends an error signal to the AVR, the consequence of which is to reduce the AVR voltage reference. This reduces the generator output voltage to bring the volt/hertz ratio back to the allowed limit. The volt/hertz limiter does not modify the generator speed or frequency value.
4. An UEL and a volt/hertz limiter oppose each other. One has a tendency to increase the generator output voltage, the other one works to reduce it. Situations could develop where the AVR will send opposite error signals, resulting in oscillations in the generator output voltage.
5. The limiters normally embedded in the AVR are not effective in a manual mode of operation of a generator excitation system. The corresponding protection will be removed unless there is a backup independent of the AVR. The UEL will be lost during manual mode because it does not have normally a backup.
6. When coordinating the loss-of-field characteristic with the UEL, remember that static or steady-state coordina-

tion is not a guarantee for proper dynamic coordination. A slow-acting UEL could lead to the infringement of the LOF characteristic during a network disturbance.

7. Conditions could develop where the stability limits of a generator with an AVR could be worse than the manual SSSL. In some situations, manual operation could never occur. The use of the manual SSSL in protection studies should be revisited and re-assessed. Simple techniques to derive the stability limits of generator-systems are needed and should be developed by standard bodies.

VII. Appendix A: K Constants Calculation Principles

The generator model used in this paper is the same as the one in [13]. Assuming the following simplification: no amortisseur windings (which normally increase the damping effect), armature resistance neglected, no "dψ/dt" terms in generator equations and no saturation, the synchronous generator can be modeled using the following equations:

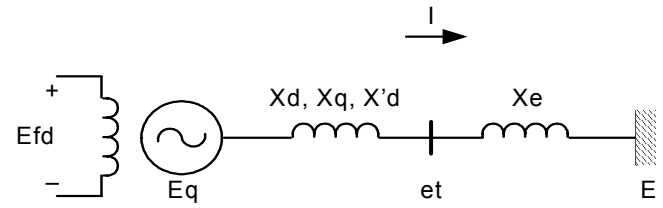

Fig. A1. Elementary power system

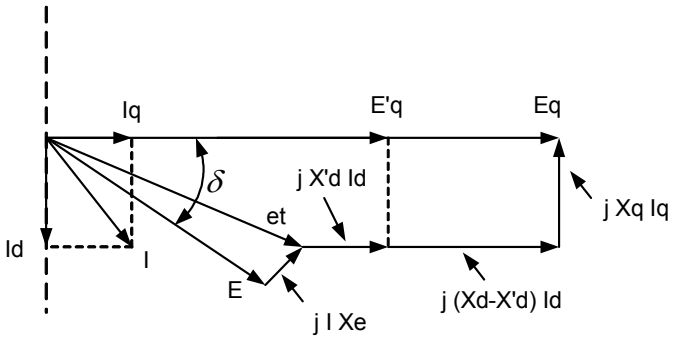

Fig. A2. Elementary power circuit vector diagram

$$e_t^2 = e_d^2 + e_q^2$$

$$-e_d = \psi_q = -X_q\, i_q$$

$$e_d = \psi_d = E_q^{'} - X_d^{'}\, i_d$$

$$E_q = E_q^{'} + (X_q - X_d^{'}) i_d$$

$$T_e = E_q\, i_q$$

$$i_d = (E_q - E\cos\delta)\frac{(X_e + X_q)}{r_e^2 + (X_e + X_q)^2} - E\sin\delta\frac{r_e}{r_e^2 + (X_e + X_q)^2}$$

$$i_q = (E_q - E\cos\delta)\frac{r_e}{r_e^2 + (X_e + X_q)^2} + E\sin\delta\frac{(X_e + X_q)}{r_e^2 + (X_e + X_q)^2}$$

$$E_q^{'} = X_{ad}\, I_{fd} - (X_d - X_d^{'}) i_d$$

$$T_{do}^{'}(dE_q^{'}/dt) = E_{fd} - X_{ad}\, I_{fd}$$

$$T_m - T_e = M\left[d(s\delta)/dt\right]$$

For small variations of the three variables Δet, $\Delta E'_q$ and $\Delta\delta$, the following relations can be derived:

$$\Delta e_t = K_5\, \Delta\delta + K_6\, \Delta E_q^{'}$$

$$\Delta E_q^{'} = \frac{K_3\, \Delta E_{fd}}{1 + s K_3\, T_{do}^{'}} - \frac{K_3\, K_4\, \Delta\delta}{1 + s K_3\, T_{do}^{'}}$$

$$\Delta T_e = K_1\, \Delta\delta + K_2\, \Delta E_q^{'}$$

For the point of operation defined by e_{to}, P_o, and Q_o, the steady-state values do, E_{qo}, E_o, e_{do}, e_{qo}, i_{do}, and i_{qo} can be calculated as:

$$I_{po} = \frac{P_o}{e_{to}}$$

$$I_{qo} = \frac{Q_o}{e_{to}}$$

$$E_{qo} = \sqrt{(e_{to} + I_{qo} X_q)^2 + (I_{po} X_q)^2}$$

$$E_o = \sqrt{(e_{to} - I_{qo} X_e)^2 + (I_{po} X_e)^2}$$

$$\sin\delta_o = \frac{e_{to} I_{po} (X_q + X_e)}{E_{qo}\, E_o}$$

$$\cos\delta_o = \frac{e_{to}\left[e_{to} - I_{qo}(X_q - X_e)\right] - X_e\, X_q (I_{po}^2 + I_{qo}^2)}{E_{qo}\, E_o}$$

$$\cos\delta_o = \frac{e_{to}\left[e_{to} - I_{qo}(X_q - X_e)\right] - X_e\, X_q (I_{po}^2 + I_{qo}^2)}{E_{qo}\, E_o}$$

$$i_{qo} = \frac{I_{po}(e_{to} + I_{qo} X_q) - I_{qo} I_{po} X_q}{E_{qo}}$$

$$i_{do} = \frac{I_{po}^2 X_q + I_{qo}(e_{to} + I_{qo} X_q)}{E_{qo}}$$

$$e_{qo} = \frac{e_{to}(e_{to} + I_{qo}X_q)}{E_{qo}}$$

$$e_{do} = i_{qo}X_q$$

The six constants K_1 to K_6 in the previous three equation constants appearing in the model are defined as follows [13]:

$K_1 = \left.\frac{\Delta T_e}{\Delta\delta}\right|_{E'_q}$ — Ratio of the change in the electrical torque over the change in the rotor angle when the flux linkages in the d axis is constant

$K_2 = \left.\frac{\Delta T_e}{\Delta E'_q}\right|_{\delta}$ — Ratio of the change in the electrical torque over the change in the flux linkages in the d axis when the rotor angle is constant

$K_3 = \frac{X'_d + X_e}{X_d + X_e}$ — Impedance factor. Formula shown when the external impedance is a pure reactance

$K_4 = \frac{1}{K_3}\frac{\Delta E'_q}{\Delta\delta}$ — Demagnetizing effect of a change in rotor angle

$K_5 = \left.\frac{\Delta e_t}{\Delta\delta}\right|_{E'_q}$ — Ratio of the change in terminal voltage over the change in rotor angle with constant E_q', the voltage proportional to the direct axis flux linkages

$K_6 = \left.\frac{\Delta e_t}{\Delta E'_q}\right|_{\delta}$ — Ratio of change in terminal voltage over the change in E_q' for constant rotor angle

The six constants, K_1 to K_6, can be computed mathematically as:

$$K_1 = \frac{X_q - X'_d}{X_e + X'_d} i_{qo} E_o \sin\delta_0 + E_{qo}E_o \cos\delta_0 \frac{E_{qo}E_o \cos\delta_0}{X_e + X_q}$$

$$K_2 = \frac{E_o \sin\delta_0}{X_e + X'_d}$$

$$K_3 = \frac{X'_d + X_e}{X_d - X_e}$$

$$K_4 = \frac{X_d - X'_d}{X_e + X'_d} i_{qo} E_o \sin\delta_0$$

$$K_5 = \frac{X_q}{X_e + X_q}\frac{e_{do}}{e_{to}} E_o \cos\delta_0 - \frac{X'_d}{X_e + X'_d}\frac{e_{qo}}{e_{to}} E_o \sin\delta_0$$

$$K_6 = \frac{X_e}{X_e + X'_d}\frac{e_{qo}}{e_{to}}$$

VIII. Appendix B: Routine to Generate the Stability Limit of a Regulated Generator Using MATLAB Language

The next listing in MATLAB language allows plotting the stability limit of a generator with an AVR using the author's method based on the matrix A eigenvalues real part becoming negative. When processed as listed, the routine will plot the stability limit appearing in Fig. 23 with the AVR gain equal to 10. Adapting the routine to the PSS case is straightforward.

```
M=3;Td0=6;Ke=10;Te=0.05;
Xd=1.6;Xq=1.55;Xpd=0.32;Xe=0.4;re=0;et0=1.0;
m=1;k=0.02;Q=-2.1;FORW=1;

while (FORW==1) | ((FORW==0) & (k > 0.01));
   while ((Q < 3) & (FORW==1)) |  ((k > 0.01) &
(FORW==0))
      PP(m)=k;
      P=PP(m);
      if FORW==1
         Q=-2.1;
      else
         Q=3;
      end
      Test=0;
      while ((Test==0) & (Q < 3) & (FORW==1)) |
((Test==0) & (k > 0.01) & (FORW==0))
         if FORW==1
            Q=Q+0.01;
         else
            Q=Q-0.01;
         end
         et0=abs(et0);
         Ip0=P/et0;
         Iq0=Q/et0;
         Eq0=sqrt((et0+Iq0*Xq)^2+(Ip0*Xq)^2);
         E0=sqrt((et0-Ip0*re-Iq0*Xe)^2+(Ip0*Xe-
Iq0*re)^2);
         sind0=(et0*Ip0*(Xq+Xe)-re*Xq*(Ip0^2+Iq0^2)-
et0*Iq0*re)/(Eq0*E0);
         cosd0=(1/(Eq0*E0))*(et0*(et0+Iq0*(Xq-Xe)-
Ip0*re)-Xe*Xq*((Ip0^2)+(Iq0^2)));
         iq0=(1/Eq0)*(Ip0*(et0+Iq0*Xq)-Iq0*Ip0*Xq);
         id0=(1/Eq0)*((Ip0^2)*Xq+Iq0*(et0+Iq0*Xq));
         eq0=et0*((et0+Iq0*Xq)/Eq0);
         ed0=iq0*Xq;

         A=(re^2)+(Xe+Xpd)*(Xq+Xe);

K1=(Eq0*E0/A)*(re*sind0+(Xe+Xpd)*cosd0)+(iq0*E0/
A)*((Xq-Xpd)*(Xe+Xq)*sind0-re*(Xq-Xpd)*cosd0);
         K2=(re*Eq0/A)+iq0*(1+(Xe+Xq)*(Xq-Xpd)/A);
         K3=1/(1+(Xe+Xq)*(Xd-Xpd)/A);
         K4=(E0*(Xd-Xpd)/A)*((Xe+Xq)*sind0-
re*cosd0);

K5=(ed0/et0)*(Xq/A)*(re*E0*sind0+(Xe+Xpd)*E0*cosd
0)+(eq0/et0)*(Xpd/A)*(re*E0*cosd0-
(Xe+Xq)*E0*sind0);
         K6=(eq0/et0)*(1-
Xpd*(Xe+Xq)/A)+(ed0/et0)*Xq*(re/A);
```

```
        A3=[0 377 0 0;-K1/M 0 -K2/M 0;-K4/Td0 0 -
1/(K3*Td0) 1/(Td0); -(Ke*K5)/Te 0 -Ke*K6/Te -1/Te];
        H3=eig(A3);
        x1=real(H3(1,1));
        x2=real(H3(2,1));
        x3=real(H3(3,1));
        x4=real(H3(4,1));

        Test= (x1 < 0) & (x2 < 0) & (x3 < 0) & (x4 < 0);
      end
if FORW==1 & Q > 2.8
        m=m-2;
        k=k-0.02;
      else
        QQ(m)=Q;
      end
      m=m+1;

      if FORW==1
        k=k+0.01;
      else
        k=k-0.01;
      end
    end
    FORW=0;
end

plot(PP,QQ)
grid
```

IX. References

[1] D. Reimert, *Protective Relaying for Power Generation Systems*, Boca Raton: CRC Press, 2006.

[2] P. Kundur, *Power System Stability and Control*, New York: McGraw-Hill, 1994.

[3] J. R. Ribero, "Minimum Excitation Limiter Effects on Generator Response to System Disturbances," IEEE Transactions on Energy Conversion, Vol. 6, No. 1, March 1991.

[4] S. S. Choy and X. M. Xia, "Under excitation limiter and its role in preventing excessive synchronous generator stator end-core heating," IEEE Trans. Power Syst., vol. 15, no. 1, pp. 95–101, February 2000.

[5] Working Group J5 of Power System Relaying Committee, Charles J. Mozina, Chairman, "Coordination of Generator Protection with Generator Excitation Control and Generator Capability", IEEE PES General Meeting, June 2007, Tampa, Fl.

[6] S. B. Farnham and R. W. Swarthout, "Field excitation in relation to machine and system operation," AIEE Trans., vol. 72, pt. III, no. 9, pp. 1215–1223, Dec. 1953.

[7] IEEE Power Engineering Society, IEEE Tutorial on the Protection of Synchronous Generators, 95 TP 102.

[8] Guide for AC Generator Protection, IEEE Standard C37.102/D7–200X, April 2006.

[9] Requirements for Cylindrical Rotor Synchronous Generators, 1989. ANSI Std. C50.13–1989.

[10] Standard for Requirements for Salient-Pole Synchronous Generators and Generator/Motors for Hydraulic Turbine Applications, 1982. ANSI Std. C50.12–1982.

[11] IEEE Recommended Practice for Excitation System Models for Power system Stability Studies, IEEE standard 421.5-1992.

[12] IEEE Task Force on Excitation Limiters, "Underexcitation Limiter Model for Power System Stability studies", IEEE Trans. On Energy Conversion, Vol. 10, No. 3, September 1995.

[13] F. P. DeMello and C. Concordia, "Concepts of synchronous machine stability as affected by excitation control," IEEE Trans. Power App. Syst., vol. PAS–88, No. 4, pp. 316–329, April 1969.

[14] C. K. Seetharaman, S. P. Verma, and A. M. El-Serafi, "Operation of synchronous generators in the asynchronous mode," IEEE Trans. Power App. Syst., vol. PAS–93, pp. 928–939, 1974.

[15] C. R. Mason, "A new loss of excitation relay for synchronous generators," AIEE Trans., vol. 68, pt. II, pp. 1240–1245, 1949.

[16] J. Berdy, "Loss-of excitation protection for modern synchronous generators," General Electric Co. Document GER-3183.

[17] R. Sandoval, A. Guzmán, H. J. Altuve, "Dynamic simulations help improve generator protection," 33rd Annual Western Protective Relay Conference, Spokane, WA, October 17-19, 2006.

[18] Carson W. Taylor, *Power System Voltage Stability*, McGraw Hill International editions 1994.

[19] The MathWorks, *MATLAB The language of Technical Computing*, Using MATLB, Version 6, November 2000.

X. Biography

Gabriel Benmouyal, P.E., received his B.A.Sc. in Electrical Engineering and his M.A.Sc. in Control Engineering from Ecole Polytechnique, Université de Montréal, Canada, in 1968 and 1970, respectively. In 1969, he joined Hydro-Québec as an Instrumentation and Control Specialist. He worked on different projects in the field of substation control systems and dispatching centers. In 1978, he joined IREQ, where his main field of activity has been the application of microprocessors and digital techniques for substation and generating-station control and protection systems. In 1997, he joined Schweitzer Engineering Laboratories, Inc. in the position of Principal Research Engineer. He is a registered professional engineer in the Province of Québec, is an IEEE Senior Member, and has served on the Power System Relaying Committee since May 1989. He holds over six patents and is the author or co-author of several papers in the field of signal processing and power networks protection and control.